EBioMedicine 15 (2017) 173–183

Contents lists available at ScienceDirect

EBioMedicine

journal homepage: www.ebiomedicine.com

Research Paper

Chronic Over-expression of Fibroblast Growth Factor 21 Increases Bile Acid Biosynthesis by Opposing FGF15/19 Action

Jun Zhang [a], Jamila Gupte [a], Yan Gong [a], Jennifer Weiszmann [a], Yuan Zhang [c], Ki Jeong Lee [b], William G. Richards [b], Yang Li [a,*]

[a] Amgen Inc., 1120 Veterans Blvd., South San Francisco, CA 94080, United States
[b] Amgen Inc., One Amgen Center Drive, Thousand Oaks, CA 91320, United States
[c] Department of Pharmacology, UT Southwestern Medical Center, 6001 Forest Park Rd, Dallas, TX 75390, United States

ARTICLE INFO

Article history:
Received 6 September 2016
Received in revised form 22 December 2016
Accepted 22 December 2016
Available online 24 December 2016

Keywords:
FGF21
FGF19
βKlotho
FGFR4
Bile acid metabolism

ABSTRACT

Pharmacological doses of fibroblast growth factor (FGF) 21 effectively normalize glucose, lipid and energy homeostasis in multiple animal models with many benefits translating to obese humans with type 2 diabetes. However, a role for FGF21 in the regulation of bile acid metabolism has not been reported. Herein, we demonstrate AAV-mediated FGF21 overexpression in mice increases liver expression of the key bile acid producing enzyme, *Cyp7a1*, resulting in an increased bile acid pool. Furthermore, in cholecystectomized mice, FGF21-mediated bile acid pool increase led to increased transit of bile acids into colon. We elucidate that the mechanism of FGF21 induced bile acid changes is mainly through antagonizing FGF15/19 function on liver βKlotho/FGFR4 receptor complex; thus inhibiting FGF15/19-mediated suppression of *Cyp7a1* expression. In conclusion, these data reveal a previously unidentified role for FGF21 on bile acid metabolism and may be relevant to understand the effects of FGF21 analogs in clinical studies.

1. Introduction

Fibroblast growth factor (FGF) 15/19 (orthologs in rodent and human, respectively) and FGF21 belong to a distinct subfamily of FGFs that play important roles in metabolic regulation (Kharitonenkov et al., 2005; Coskun et al., 2008; Tomlinson et al., 2002). Their effects on glucose and lipid homeostasis are interchangeable. Pharmacological studies with both molecules demonstrated comparable efficacy in lowering serum glucose, triglyceride (TG), and cholesterol levels, improving insulin sensitivity and reducing body weight in many diabetic disease rodent and non-human primate models (Fu et al., 2004; Kharitonenkov et al., 2007; Xu et al., 2009a). Both FGF15/19 and FGF21 activate FGF receptors (FGFRs) in the context of the co-receptor, βKlotho, a single-pass transmembrane protein with two homologous extracellular domains (Wu et al., 2007; Kurosu et al., 2007; Ogawa et al., 2007; Ding et al., 2012; Wu et al., 2008; Lin et al., 2007).

Despite common pharmacological outputs on glucose and lipid metabolism, differences exist between FGF15/19 and FGF21. The ability of FGF15/19 to activate FGFR4, the predominant receptor expressed in the liver, has been linked to its regulation of bile acid (BA) homeostasis (Wu et al., 2007; Yang et al., 2012). FGF15/19 signals from the intestine to the liver through the βKlotho/FGFR4 complex to suppress the expression of the rate-limiting enzyme of bile acid synthesis, cholesterol 7α-hydroxylase (*Cyp7a1*), as part of a negative feedback loop on bile acid synthesis in liver (Holt et al., 2003; Inagaki et al., 2005; Wu et al., 2011). Although other pathways are also involved in regulating bile acid biosynthesis, the FGF15/19-βKlotho/FGFR4 axis is critical in maintaining bile acid homeostasis. Mice deficient in *Fgf15*, *Fgfr4*, or *βKlotho* all exhibit elevated hepatic *Cyp7a1* mRNA expression, fecal BA excretion, and BA pool size (Ito et al., 2005; Yu et al., 2000; Ge et al., 2014) demonstrating the critical role of FGF15/19 in maintaining the feedback regulation of BA synthesis. Contrary to FGF15/19, FGF21 is unable to activate βKlotho/FGFR4 (Kurosu et al., 2007; Wu et al., 2009; Yang et al., 2012; Ge et al., 2012), and accordingly has yet to be identified as a regulator of BA metabolism.

However, in our studies to understand FGF21 function, we observed that AAV-mediated FGF21 overexpression actually increased *Cyp7a1* expression and bile acid synthesis in the liver, resulting in a significant increase in bile acid pool size. Mechanism of action studies suggest that the observed increases in bile acid synthesis by FGF21 treatment is, at least in part, due to the shared binding site between FGF21 and FGF15/19 on co-receptor βKlotho, whereby FGF21 reverses the inhibition of bile acid synthesis by acting as an antagonist to FGF15/19 function. Our results provide evidence of cross-talk between endocrine FGFs, and reveal a pharmacological action of FGF21 in regulating bile acid homeostasis.

* Corresponding author at: Department of Cardiometabolic Disorders, Amgen Inc., 1120 Veterans Blvd., South San Francisco, CA 94080, United States.
E-mail address: yangl@amgen.com (Y. Li).

http://dx.doi.org/10.1016/j.ebiom.2016.12.016

2. Materials and Methods

2.1. Animal Housing and Care

Animal housing conditions and research protocols were approved by the Amgen Institutional Animal Care and Use Committee (IACUC). Mice were housed in a specified-pathogen free, AAALAC, Intl-accredited facility in ventilated microisolators. Procedures and housing rooms are positively pressured and regulated on a 12:12 dark:light cycle. All animals received reverse-osmosis purified water ad libitum via an automatic watering system. FGFR4 KO mice and WT littermates were generated as described earlier (Ge et al., 2014). C57BL/6J animals (The Jackson Laboratory) were singly housed and fed standard chow (2020× Teklad global soy protein-free extruded rodent diet; Harlan). For diet-induced obese (DIO) animal studies, 16–18-week-old C57BL/6J male mice fed a 60 kcal% fat diet (D12492, Research Diets) for 10 weeks were purchased from the Jackson Laboratory.

Cholecystectomy was performed on 16–18 week old DIO animals at the Jackson Laboratory. In brief, after animals were treated with surgical anesthesia, excision of the gallbladder and ligature of the cystic duct and attached artery were performed. Animals were monitored for recovery before shipment.

For studies with protein injection, mice were intraperitoneally (i.p.) injected with recombinant FGF19 or human FGF21 protein (at 1 mg/kg body weight in 0.2 ml PBS) or an equal volume of PBS as a control.

2.2. Fasting Glucose, Insulin, Cholesterol and TG Measurements

Mice were fasted for 4 h beginning at 6 AM on the day of the experiment. Blood samples obtained from the tail vein were used for fasting glucose and cholesterol measurement. Fasting blood glucose was measured by AlphaTrak glucometer (Abbott). Insulin content was determined by using Insulin (mouse) ultra-sensitive EIA kit (80-INSMSU-E10, ALPCO Diagnostics). For tissue cholesterol and TG measurements, 40–50 mg of liver tissues were homogenized by Qiagen tissue lyzer for 30 s to 1 min and then extracted by chloroform/methanol (2:1 v/v). After washing with 0.5 ml of 50 mM NaCl and 0.5 ml of 0.36 M $CaCl_2$/Methanol, organic phase was saved for further measurement. Serum and tissue cholesterol and TG were measured by Infinity ™ Total Cholesterol Reagent (TR13421, Thermo Scientific) and Infinity ™ Triglyceride Reagent (TR22321, Thermo Scientific), respectively.

2.3. Feces and Tissue Bile Acids Analysis

Bile acids were measured enzymatically using the mouse total bile acid assay kit (80470, Crystal Chem). To determine fecal bile acid excretion, the feces from individually housed mice were collected, dried, and weighed over a 5–7 day period. Dried feces were then minced and extracted in 10 ml/g of 75% ethanol at about 50 °C for 2 h. The extract was centrifuged, and 1 ml samples of supernatant were diluted to 4 ml with a 25% PBS solution for the assay. The bile acid concentration was measured enzymatically, a measurement of buffer only without the extract was used as the background and subtracted from the measurement of each sample. Fecal bile acid content (μmol/100 g of body weight or μmol/animal) was used to represent bile acid excretion.

The total bile acid pool size was determined as bile acid content of the liver, gallbladder, and small intestine and its contents. After the mice were weighed, anesthetized, and exsanguinated, the fresh organs were collected, minced together, and extracted in 15 ml of 75% ethanol at about 50 °C for 2 h. The extract was centrifuged, 1 ml samples of supernatant for the assay were diluted to 4 ml with 75% ethanol, and then 1 ml diluted samples were further diluted to 4 ml with 25% PBS. Bile acids were determined enzymatically, a measurement of buffer only without the extract was used as the background and subtracted from the measurement of each sample. The pool size was expressed as micromoles of bile acid/100 g of body weight or μmol/animal.

2.4. AAV Preparation

Recombinant adeno-associated virus (AAV) expressing mouse FGF15 or mouse FGF21 were produced by transient transfection into HEK293T cells using helper-free system, purified by gradient centrifugation, buffer exchanged. 1×10^{11}–1×10^{12} virus particles per mouse in PBS expressing FGF15, FGF21 (under the control of EF1a promoter) or an empty vector as negative control were intravenously (i.v.) injected into mice through the tail vein.

2.5. FGF15 and FGF21 ELISA

Microtiter plates were coated with 2.0 μg/ml of sheep anti-mouse FGF15 (AF76755, R&D Systems) or goat anti-mouse FGF21 (AF3057, R&D Systems) in PBS overnight at 4 °C, and then washed one time with PBS. The plates were then blocked with 3% BSA in PBS for 1 h at room temperature followed by a two-time wash with PBS + 0.01% Tween-20 (PBST). Serum samples, diluted in PBS + 1% BSA, were added to the plates and incubated overnight at 4 °C followed by 3 washes with PBST. Biotinylated antibodies in PBS + 1% BSA were added and incubated for 1 h at room temperature. Streptavidin-conjugated HRP was then added and incubated for 20 min. The plates were washed 6 times with PBS + 0.01% Tween-20 and developed with tetramethyl benzidine (TMB) as substrate. 1 N HCl was added as the stop solution. The results were read on a SpectraMax plate reader (Molecular Devices) at 450 and 550 nm. Recombinant FGF15 and FGF21 proteins (R&D Systems) were used for standard curve.

2.6. Quantitative RT-PCR (RT-qPCR)

Mouse tissue total RNA was isolated using QIAcube and RNeasy kit (Qiagen). 8 ng of isolated total RNA was used as starting material. The reactions were performed in duplicate on the BioMark™ HD System according to the manufacturer's protocol. Relative mRNA levels were calculated by the comparative threshold cycle method using four housekeeping genes as the internal controls. The primer and probes sets were ordered from IDT: *Cyp7a1* (Mm.PT.56a.17448793); *Cyp27a1* (Mm.PT.56a.42377566); *Cyp7b1* (Mm.PT.56a.31179802); *Cyp8b1* (Mm.PT.56a.12268653.g); *Hmgcr* (Mm.PT.56a.13325212); *Srebp1c* (Mm.PT.56a.42313188); *Asbt* (Mm.PT.56a.41743474); *Osta* (Mm.PT.56a.17102339); *Ostb* (Mm.PT.56a.23668920); *Abcg5* (Mm.PT.56a.8809476); *Abcg8* (Mm.PT.56a.7910478); *Bsep* (Mm.PT.56a.43710058); *Mrp2* (Mm.PT.56a.5554359); *Ntcp* (Mm.PT.56a.43000030); *Oatp1* (Mm.PT.56a.32911698); *Oatp4* (Mm.PT.56a.30581202); *Mrp3* (Mm.PT.56a.28882380); *Mrp4* (Mm.PT.56a.23407634.g).

2.7. Solid-phase Binding Assay

Nunc Maxisorp 96-well plates were coated overnight at 4 °C with 50 μl of 2 μg/ml AffiniPure rabbit anti-human IgG, Fcγ fragment specific antibody (Jackson ImmunoResearch). Plates were washed 4 times with PBS containing 0.05% Tween-20 and then blocked with PBS containing 3% BSA for 2 h at room temperature. Following another wash, 100 μl of 1 μg/ml human FGFR4-Fc was added and the plates were incubated for 1 h at room temperature. Plates were washed again and 45 μl of 0.5 μg/ml His-tagged soluble recombinant human βKlotho protein was added to each well. After 1.5 h, biotinylated FGF19 (using Pierce Sulfo-NHS-LC-Biotin) and unlabeled human FGF21 or FGF23 were added and the plates were incubated for another 1.5 h at room temperature. The plates were then washed and streptavidin-HRP (R&D Systems) was added for 30 min. After washing, TMB Reagent (BD Biosciences) was added and absorbance at 450 nm was read on SpectraMax.

2.8. Cell Culture and Transfections

L6 myoblast cells were maintained in DMEM (Mediatech) medium supplemented with 10% FBS (Invitrogen) and 1× penicillin/streptomycin (Invitrogen). Cells were transfected with expression vectors using the Lipofectamine 2000 transfection reagent (Invitrogen) according to the manufacturer's protocol.

2.9. MSD Analysis of pERK Activation

L6 cells (8×10^3 cells per well) were transfected with βKlotho and FGFR4 in 96-well plates and serum-starved overnight the day after transfection. Following treatment with various concentrations of FGF proteins for 15 min, cells were snap-frozen in liquid nitrogen. Cell lysates were prepared by thawing the plates at 4 °C and adding 70 μl of complete MSD lysis buffer with 0.1% SDS to each well. Plates were shaken at 4 °C for 30 min on an orbital shaker. 25 μl of cell lysate was transferred to wells of Phospho/Total ERK1/2 Whole Cell Lysate plates (Meso Scale Discovery) and pERK and Total ERK were measured according to the manufacturer's protocol.

3. Results

3.1. Both FGF15 and FGF21 Regulate Bodyweight, Glucose, and Bile Acid Synthesis In Vivo

We utilized recombinant adeno-associated virus (AAV) as a gene delivery approach to overexpress FGF15 and FGF21, to study their functions *in vivo*. Both normal chow diet (Fig. 1) and DIO (Fig. 2) mice were injected with either AAV expressing FGF15, FGF21, or AAV containing an empty vector (EV) as the negative control. At week 2 post AAV injection, both animal models displayed the similar expected metabolic changes including reduced body weight, fasting glucose, insulin, and decreased plasma triglyceride (TG) and cholesterol levels (Figs. 1A and 2A). Serum FGF15 and FGF21 levels in the injected animals reached 4000 ng/ml and 300 ng/ml, respectively (Fig. S1). As reported previously (Inagaki et al., 2005), FGF15 also lowered bile acid pool in both normal chow and high fat diet (HFD) fed animals (Figs. 1A and 2A). Unexpectedly, in both animal models we found that in contrast to FGF15, FGF21 significantly increased bile acid pool (Figs. 1A, 2A, Figs. S2A and S2B). The bile acid pool includes the combined bile acid contents collected from the liver, gallbladder, and small intestine. The bile acid levels in individual tissues as well as colon and feces (collected over a 5 to 7-day period) are depicted separately in Figs. 1B, 2B, and Fig. S2. The small intestine holds the majority (>90%) of the bile acid pool. FGF15 overexpression significantly decreased small intestinal bile acid content and excreted fecal bile acid levels in chow fed animals. In contrast, FGF21 overexpression resulted in a significant increase in the liver and small intestinal bile acid level (Fig. 1B, Fig. S2), while in DIO animals FGF21 overexpression also resulted in either a trended or a significantly increased gallbladder and excreted fecal bile acid contents without or with normalization to body weight, respectively (Fig. 2B, Fig. S2). Because the positive effect of FGF21 on increased bile acid pool had not been reported, we sought to further understand the underlying mechanism for this observation. Since both chow fed and DIO models presented similar effects from both FGF15 and FGF21, we decided to focus on chow fed animals to further explore the mechanism of FGF21 regulated bile acid metabolism.

3.2. FGF15 and FGF21 Regulate Genes Involved in Bile Acid Synthesis and Transport

To understand how FGF21 regulates bile acid metabolism, we assessed the genes involved in bile acid homeostasis in both liver and ileum. There are two bile acid biosynthetic pathways in the liver: the classic and the alternative; the former contributing to ~75% of overall BA synthesis in mice (Russell and Setchell, 1992; Thomas et al., 2008). Cholesterol 7α-hydroxylase (CYP7A1) catalyzes the first and rate-limiting step in the classic BA synthetic pathway (Myant and Mitropoulos, 1977). It is well established that CYP7A1 is tightly regulated by a negative feedback loop mediated by FGF15/19 (Holt et al., 2003; Inagaki et al., 2005; Wu et al., 2009). In AAV-FGF15 treated animals, *Cyp7a1* mRNA levels were significantly reduced, consistent with published reports. No significant changes to *Cyp27a1*, *Cyp7b1* (two key enzymes in the alternative pathway of BA synthesis) and *Cyp8b1* were observed upon FGF15 treatment. In contrast, FGF21 overexpression led to significant up-regulation of both *Cyp7a1* and *Cyp27a1* expression (Figs. 1C and 2C). *Cyp7b1* expression was reduced in the FGF21-treated normal chow group but unchanged in DIO animals (Figs. 1C and 2C). No significant changes were noted for sterol regulatory element-binding protein 1c (*Srebp1c*) and a trended increase in the cholesterol synthetic gene, 3-hydroxy-3-methyl-glutaryl-CoA reductase (*Hmgcr*) mRNA levels were observed in the liver of chow fed mice (Fig. 1C). Thus, these results suggest that the primary cause of the increased bile acid pool size in FGF21 treated animals is due to increased bile acid synthesis.

To further characterize the role of FGF21 in bile acid metabolism, we profiled the expression of hepatic and ileum membrane transporters known to play critical roles in maintaining bile acid and sterol homeostasis. The two genes, *Abcg5* and *Abcg8*, which heterodimerize to form a cholesterol efflux transporter, demonstrated the most significant change in the liver upon FGF15 and FGF21 treatment (Figs. 1C and 2C). To a much lesser magnitude, expression of the bile salt export pump, *Bsep* (*Abcb11*), at the canalicular membrane of hepatocytes was down-regulated by FGF15 and up-regulated by FGF21 in chow fed animals. Along with increased synthesis of bile acid in the hepatocytes resulting from increased *Cyp7a1* expression, this suggests an increased excretion of cholesterol and bile salt from liver of FGF21 treated animals, consistent with the observed increased bile acid levels in the gallbladder and small intestine (Figs. 1B and 2B). Expression of the three transporters involved in portal bile acid uptake, *Ntcp*, *Oatp1* (*Slc21a1*), and *Oatp4* (*Slca10*), were up-regulated by both FGF15 and FGF21. *Mrp3* (*Abcc3*) and *Mrp4* (*Abcc4*), located on the basolateral membrane important for systemic efflux of bile acids, were not affected by FGF15 or FGF21 treatment. In ileum, FGF15 and FGF21 mildly induced expression of the apical sodium-dependent bile acid transporter, *Asbt* (*Slc10a2*). While FGF15 mildly reduced expression of the organic solute transporter *Ostα*/*Ostβ*, and *Abcg5*/*Abcg8*, FGF21 did not affect *Abcg5*/*Abcg8* and slightly increased the *Ostβ* mRNA level (Figs. 1C and 2C). Together, these data demonstrate that both FGF15 and FGF21 regulate key genes involved in maintaining bile acid homeostasis. While the effects of FGF15 and FGF21 on key bile acid synthetic genes, such as *Cyp7a1*, differ, many genes involved in cholesterol and bile acid transport are similarly regulated by FGF15 and FGF21.

To understand if these changes were mediated by a direct or indirect action of FGF21, we performed acute studies where the gene expression changes from liver and ileum were examined 20 min, 2 h, and 5 h after a single injection of recombinant FGF19 or FGF21 proteins. Since the plasma half-life of both FGF19 and FGF21 are only ~1 h (Xu et al., 2009b; Wu et al., 2010), any effects observed from this acute treatment is most likely results from direct effects of the ligands rather than indirect effects that may require extended exposure of the ligands. As shown in Fig. 1D, no significant changes to gene expressions were observed at the 20 min time point. At 2-hour and 5-hour post injection, while FGF19 suppressed *Cyp7a1* expression as seen from the chronic treatment, FGF21 did not increase *Cyp7a1*, it actually caused a slight reduction similar to a previous report (Fig. 1E and F, Wu et al., 2011). These results suggest that the increased bile acid synthesis from a chronic FGF21 treatment may be due to an indirect mechanism. Interestingly, while most of the affected transporters observed by FGF21 chronic treatment did not show a consistent change in the acute treatments, *Abcg5* and *Abcg8* were up regulated similar to the chronic treatment suggesting that the effects of FGF19 and FGF21 on these two genes might be a direct effect (Fig. 1F).

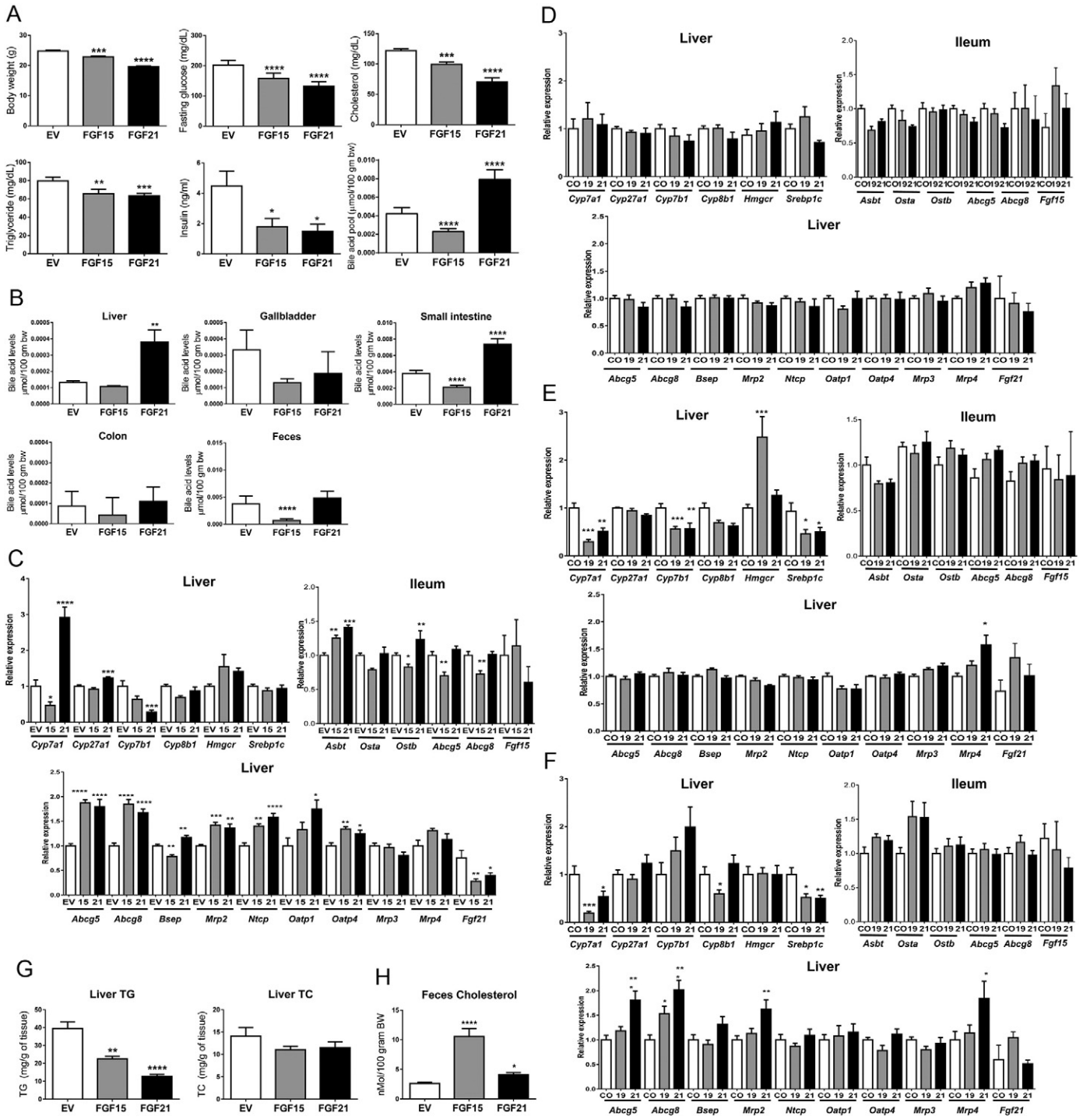

Fig. 1. FGF15 and FGF21 over-expression *in vivo* induce similar body weight and glucose lowing effects but opposite bile acid regulatory effects. 10–12 week old C57BL/6 animals were injected with AAV-empty vector (EV), AAV-FGF15 or AAV-FGF21 (n = 8 each group). (A) Body weight, fasting glucose, plasma cholesterol, triglyceride and insulin were significantly decreased at week 2 post AAV delivery. Mice treated with AAV-FGF15 showed significantly decreased total bile acid level, while AAV-FGF21 showed significantly increased total bile acid level when compared to AAV-EV treated control group. (B) Liver, gallbladder, small intestine, colon and feces bile acid levels in animals treated with AAV-EV, AAV-FGF15 and AAV-FGF21 (n = 8 each group). (C) qPCR analysis of key enzymes in bile acid synthesis and transporters in the liver and ileum. mRNA abundance was normalized by housekeeping genes and is presented as relative expression. (D–F) qPCR analysis of key enzymes in bile acid synthesis and transporters in the liver and ileum 20 min (D), 2 h (E), or 5 h (F) after FGF19 and FGF21 treatment. mRNA abundance was normalized by housekeeping genes and is presented as relative expression. (G) Liver TG and cholesterol contents. (H) Fecal cholesterol contents. $^{*}p < 0.05$, $^{**}p < 0.01$, $^{***}p < 0.001$, $^{****}p < 0.0001$.

3.3. Effects of FGF21 on Lipid Homeostasis

Since FGF21 affected the expression of cholesterol and bile acid synthesis and transport genes, we further evaluated its effects on lipid metabolism. Similar to plasma TG levels, liver TG contents were significantly reduced upon FGF15 and FGF21 treatments (Figs. 1G and 2D). Consistent with increased liver *Abcg5/Abcg8* expression, fecal cholesterol levels were increased by both FGF15 and FGF21 (Fig. 1H). Compared to the FGF21 group, the higher fecal cholesterol level in the FGF15 treatment group may be the additional effects of reduced conversion to

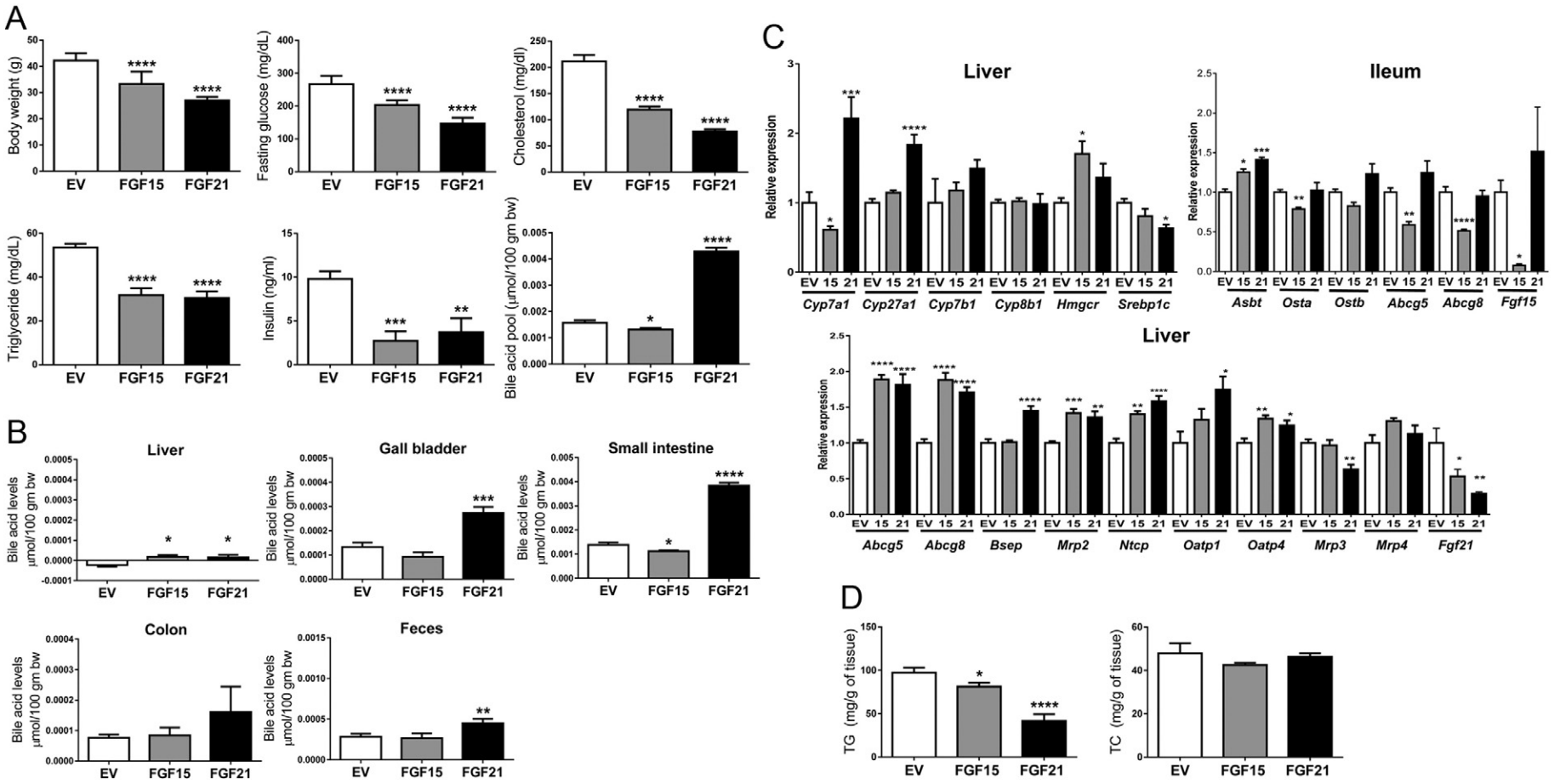

Fig. 2. Both FGF15 and FGF21 lower body weight and glucose levels in DIO animals but exhibit opposite actions on bile regulation. 16–18 week old C57BL/6 DIO animals were injected with AAV-empty vector (EV), AAV-FGF15 and AAV-FGF21 (n = 8 each group). (A) Body weight, fasting glucose, plasma cholesterol, TG, insulin were significantly decreased at week 2 post AAV delivery. Mice treated with AAV-FGF15 showed significantly decreased total bile acid level, while AAV-FGF21 showed significantly increased total bile acid level when compared to AAV-EV treated control group. (B) Liver, gallbladder, small intestine, colon and feces bile acid levels in animals treated with AAV-EV, AAV-FGF15 and AAV-FGF21. The measurements for liver are likely below the detection limit of the assay especially for the EV group, which may be the reason for the negative value after subtracting background of the assay. (C) qPCR analysis of key enzymes in bile acid synthesis and transporters in the liver and ileum. mRNA abundance was normalized by housekeeping genes and is presented as relative expression. (D) Liver TG and cholesterol contents. *$p < 0.05$, **$p < 0.01$, ***$p < 0.001$, ****$p < 0.0001$.

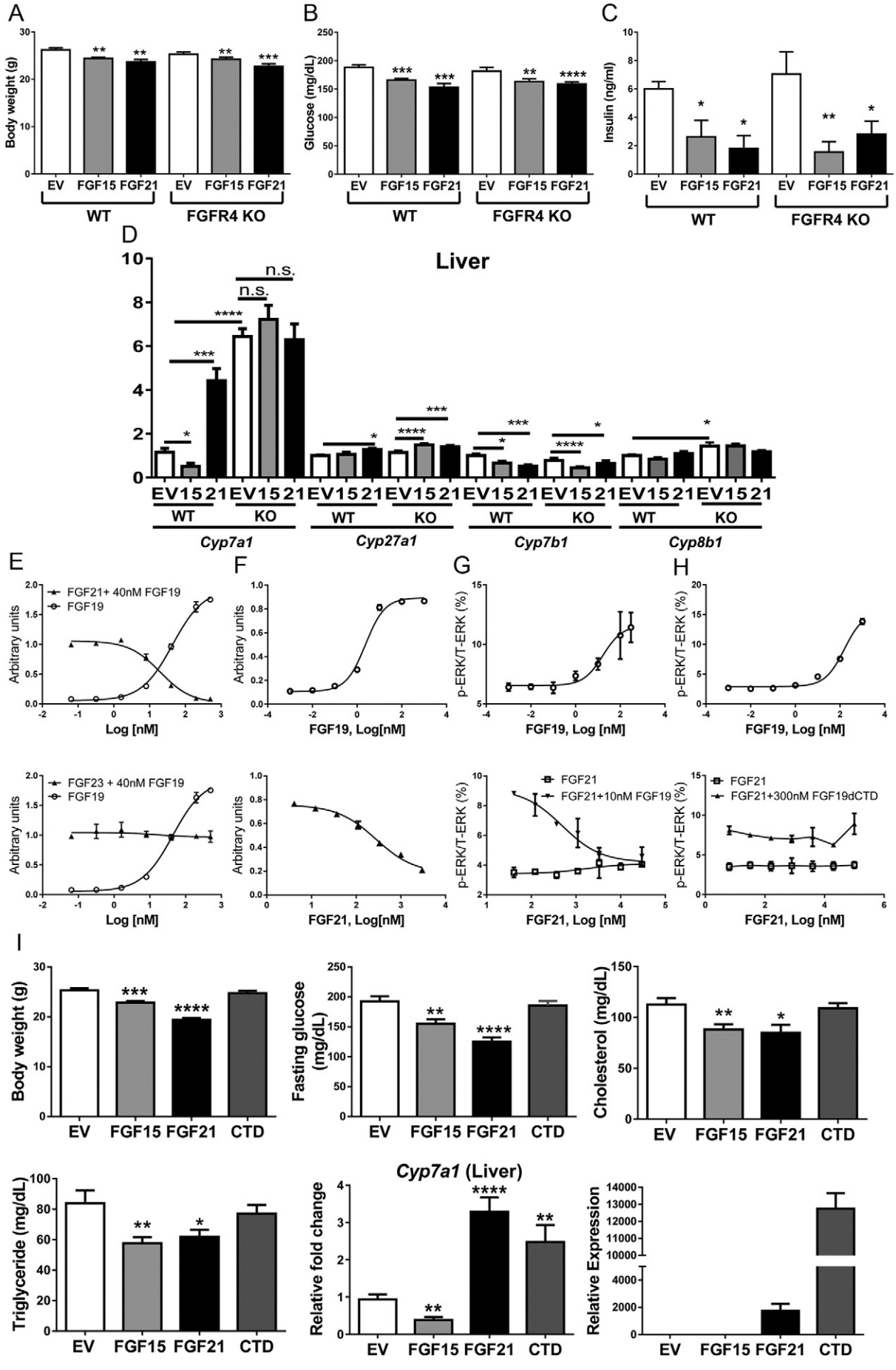
A
Body weight (g)
EV FGF15 FGF21 EV FGF15 FGF21
WT FGFR4 KO
B
Glucose (mg/dL)
EV FGF15 FGF21 EV FGF15 FGF21
WT FGFR4 KO
C
Insulin (ng/ml)
EV FGF15 FGF21 EV FGF15 FGF21
WT FGFR4 KO
D
Liver
n.s.
n.s.
EV15 21 EV15 21 EV15 21 EV15 21 EV15 21 EV15 21 EV15 21 EV15 21
WT KO WT KO WT KO WT KO
Cyp7a1 Cyp27a1 Cyp7b1 Cyp8b1
E
FGF21+ 40nM FGF19
FGF19
Arbitrary units
Log [nM]
F
Arbitrary units
FGF19, Log[nM]
G
p-ERK/T-ERK (%)
FGF19, Log [nM]
H
p-ERK/T-ERK (%)
FGF19, Log [nM]
FGF23 + 40nM FGF19
FGF19
Arbitrary units
Log [nM]
Arbitrary units
FGF21, Log[nM]
FGF21
FGF21+10nM FGF19
p-ERK/T-ERK (%)
FGF21, Log [nM]
FGF21
FGF21+300nM FGF19dCTD
p-ERK/T-ERK (%)
FGF21, Log [nM]
I
Body weight (g)
EV FGF15 FGF21 CTD
Fasting glucose (mg/dL)
EV FGF15 FGF21 CTD
Cholesterol (mg/dL)
EV FGF15 FGF21 CTD
Triglyceride (mg/dL)
EV FGF15 FGF21 CTD
Cyp7a1 (Liver)
Relative fold change
EV FGF15 FGF21 CTD
Relative Expression
EV FGF15 FGF21 CTD

bile acid and reduced absorption that resulted from lower bile acid pool levels in FGF15 overexpression animals. Despite the significantly reduced plasma cholesterol levels (Figs. 1A and 2A), liver cholesterol contents were not significantly changed with either FGF15 or FGF21 (Figs. 1G and 2D). In the case of FGF21, the increased demand for hepatic cholesterol for catabolism through both increased bile acid synthesis and ABCG5/8 mediated excretion may have resulted in a compensatory increase in the de novo synthesis and/or uptake of cholesterol-carrying lipoprotein from the blood into hepatocytes. The latter is consistent with the observed decreases in plasma total cholesterol levels in the FGF21-treated animals.

The effects observed with FGF21 treatment on bile acid and cholesterol metabolism as well as on insulin, glucose, and energy metabolism are reminiscent of the *Cyp7a1* transgenic mice (*Cyp7a1-Tg*) (Li et al., 2011a, 2010). It is interesting to speculate whether bile acids contribute to the pharmacology observed with FGF21. Since FGF21 and FGF15 have opposite effects on bile acid metabolism, yet similar effects on glucose, lipid, and energy metabolism, we believe these endocrine FGFs can regulate metabolism independent of bile acids. However, since the magnitude of effects appears stronger for FGF21 over FGF15, one cannot rule out additional bile acid mediated contributions to FGF21 in these AAV studies.

3.4. FGF21 Effects are FGFR4 Dependent

Since FGF21-induced *Cyp7a1* expression on hepatocytes does not appear to come from a direct activating signal, we questioned if FGF21 mediates this action indirectly by interfering other bile acid regulatory pathways, such as the FGF15/19/FGFR4 axis. Since FGF15/19 suppresses bile acid synthesis directly through activation of βKlotho/FGFR4 on hepatocytes, we tested the effects of FGF21 on bile acid metabolism in FGFR4 knockout (KO) mice. Thus, if FGF21 impairs the FGF15/19-FGFR4 interaction, then FGF21 would lose its effect in FGFR4 KO mice. If, however, FGF21 mediates its effect through an alternative pathway, then the absence of FGFR4 should not affect FGF21's regulation of *Cyp7a1*. The FGFR4 KO line was generated using the Zinc Finger Nuclease (ZFN) technology and its characterization has been described in detail (Ge et al., 2014). AAV-FGF15, AAV-FGF21, and AAV-EV were injected into 10–12 week old FGFR4 KO and WT age-matched littermate controls. At this age, no body weight or glucose differences were detected between WT and FGFR4 KO mice, while increased basal *Cyp7a1* was observed in FGFR4 KO (Fig. 3A–D, comparing the EV groups). Overexpression of both FGF15 and FGF21 decreased bodyweight, fasting glucose, and insulin in both genotypes (Fig. 3A–C) consistent with previous reports that glucose regulation is mainly mediated through βKlotho/FGFR1c complex but not βKlotho/FGFR4 complex (Zhang and Li, 2014). While, as previously reported, the inhibition of *Cyp7a1* by FGF15 was completely dependent on FGFR4, the ability of FGF21 to increase *Cyp7a1* expression was also abolished in FGFR4 KO mice (Fig. 3D, Inagaki et al., 2005). In comparison, the effects of FGF15 and FGF21 on the expression of *Cyp27a1*, *Cyp7b1*, and *Cyp8b1* were modest and not affected by FGFR4 KO (Fig. 3D). Since FGF21 does not directly activate FGFR4 *in vitro* or *in vivo*, and FGFR4 KO has not reached the maximal *Cyp7a1* expression levels (a FGFR4 and SHP double KO showed a higher *Cyp7a1* level than either KO alone, Kong et al., 2012), this dependency of FGF21 on FGFR4 to up-regulate *Cyp7a1* suggest a potential mechanism of FGF21 on bile acid metabolism, by affecting the FGF15/19/FGFR4 pathway.

3.5. FGF21 Competes with FGF15/19 Binding to the βKlotho/FGFR4 Receptor to Modulate Downstream Signaling

Previous studies show that the C-terminal domains (CTD) of FGF19 and FGF21 are responsible for binding to βKlotho, and FGF21-CTD inhibits FGF19 binding to recombinant βKlotho and FGF19 signaling in rat hepatoma cell line H4IIE (Wu et al., 2008; Goetz et al., 2012). This suggests that while FGF21 does not activate βKlotho/FGFR4, it may interfere with FGF15/19's ability to bind and activate βKlotho/FGFR4 receptor complex through competition at binding to βKlotho. However, on cell lines established to express a selective combination of βKlotho and FGFRs, FGF21 inhibited FGF19 binding only to βKlotho/FGFR1c but not to βKlotho/FGFR4 (Yang et al., 2012). This lack of competition reported by Yang et al. could be due to an insufficient amount of FGF21 used in their studies or an imbalanced FGFR4 and βKlotho levels. To clarify if FGF21 is able to block the binding of FGF19 to βKlotho when βKlotho is complexed with FGFR4, we established both FGFR4 dependent interaction and signaling assays. The interaction studies were performed on a solid phase ELISA binding format *in vitro*. We first tested the ability of FGF21 to compete with FGF19 binding to βKlothoECD (extracellular domain) in the absence of FGFRs. The recombinant βKlothoECD was first captured on plates, a dose dependent increase in signal was detected when increasing amounts of biotinylated FGF19 was added, indicating interaction between FGF19 and βKlotho as has been reported previously (Fig. 3E, Kurosu et al., 2007; Lin et al., 2007; Wu et al., 2007). At a fixed concentration of labeled FGF19, unlabeled FGF21, but not FGF23, was able to inhibit FGF19 signal indicating the ability of FGF21 to compete with FGF19 binding to the co-receptor (Fig. 3E). Next, we tested the effects of FGF21 on FGF19 interaction with βKlothoECD in the presence of FGFR4. Recombinant FGFR4 ECD fused with Fc (FGFR4ECD-Fc) was first captured on plates and then incubated with βKlothoECD. A dose dependent increase in signal was detected when increasing amounts of biotinylated FGF19 were added, indicating interaction between FGF19 and βKlotho/FGFR4 (Fig. 3F top panel). When unlabeled FGF21 was then added to this mixture at a fixed concentration of labeled FGF19, FGF21 was able to reduce FGF19 signal remaining on the βKlotho/FGFR4 complex (Fig. 3F bottom panel). Since FGF21 is only able to interact with βKlotho (Ogawa et al., 2007), which is retained on the plate through its interaction with FGFR4, these results suggest that FGF21 is able to block FGF19 binding to βKlotho/FGFR4 complex. To understand if FGF19 signaling through βKlotho/FGFR4 can also be inhibited by FGF21, we transfected L6 cells with βKlotho and FGFR4 and examined FGF19 mediated signaling. FGF19 induced phosphorylation of ERK (pERK) in transfected L6 cells in a dose dependent manner (Fig. 3G top panel). FGF21 did not induce

Fig. 3. FGF21 regulates bile acid synthesis by antagonizing FGF19 function. (A-D) FGF21 effects on bile acid synthesis are FGFR4 dependent. 10–12 week old FGFR4 KO and littermate control animals were injected with AAV-EV, AAV-FGF15 or AAV-FGF21 (n = 8 each group). (A) Body weight, (B) fasting glucose, and (C) insulin were significantly decreased at week 2 post AAV deliveries in both control and FGFR4 KO animals, (D) qPCR analysis of key enzymes in bile acid synthesis in the liver. mRNA abundance was normalized by housekeeping genes and is presented as relative expression. *Cyp7a1* regulation by FGF15 and FGF21 was only observed in littermate control but not FGFR4 KO animals. (E–H) FGF21 competes with FGF19 for binding to βKlotho and βKlotho/FGFR4 *in vitro* and modulates pERK signaling. (E) Recombinant βKlotho was coated on plate. FGF19 showed binding to βKlotho in a dose dependent manner. At a fixed 40 nM concentration of labeled FGF19, unlabeled FGF21, but not FGF23, inhibited FGF19 binding to βKlotho. (F) Recombinant βKlotho and FGFR4 were coated on plate. FGF19 showed βKlotho/FGFR4 binding in a dose dependent manner. An increasing amount of FGF21 was incubated with 5 nM FGF19, and a dose dependent inhibition of βKlotho/FGFR4 was observed. (G) L6 cells were transfected with expression vectors expressing hβKlotho and hFGFR4. FGF19 induced p-ERK activity in a dose dependent manner. An increasing amount of FGF21 was incubated with 10 nM FGF19, and a dose dependent inhibition of βKlotho/FGFR4 was observed. (H) L6 cells were transfected with expression vectors expressing hβKlotho and hFGFR4. FGF19dCTD induced p-ERK activity in a dose dependent manner. At a fixed 300 nM concentration of FGF19dCTD, unlabeled FGF21 did not inhibit FGF19dCTD signaling through βKlotho/FGFR4. (I) The C-terminal domain of FGF21 fails to regulate bodyweight and glucose levels *in vivo*, but maintains up-regulation of *Cyp7a1*. 10–12 week old C57BL/6 animals were injected with AAV-EV, AAV-FGF15, AAV-FGF21 or AAV-FGF21CTD (labeled as CTD, n = 8 each group). Body weight, fasting glucose, plasma cholesterol and triglyceride of AAV-FGF15 and AAV-FGF21 treated animals were significantly decreased at week 2 post AAV delivery, while AAV-FGF21 CTD did not present such effects compared to control animals. In contrast, AAV-FGF21 CTD significantly increased *Cyp7a1* expression in liver similarly to wild type FGF21. Expression of the CTD construct was verified by qPCR using a probe specific for the AAV expressed FGF21 or CTD. $^{*}p < 0.05$, $^{**}p < 0.01$, $^{***}p < 0.001$, $^{****}p < 0.0001$, ns not significant.

signaling on βKlotho/FGFR4 in transfected L6 cells but was able to block the pERK signals of 10 nM FGF19, with similar potency to that of the binding assay (Fig. 3G lower panel). As a control, we also tested a variant of FGF19 without its C-terminal domain, FGF19dCTD. FGF19dCTD does not bind βKlotho and activates FGFR4 in a βKlotho independent manner (Wu et al., 2009). In contract to its effect on wild type FGF19, FGF21 did not inhibit FGFR4 signaling activated by FGF19dCTD (Fig. 3H). These results demonstrate that FGF21 can compete with FGF19 binding to βKlotho, and act as an antagonist of FGF19-mediated signaling through βKlotho/FGFR4. The high levels of FGF21 required to achieve effective inhibition in these two assays were due to the presence of high amounts of FGF19 (Fig. 3F, G). Under physiological conditions where FGF15/19 levels are several orders of magnitude less, the levels of FGF21 required to achieve inhibition may also be significantly reduced (Ge et al., 2014; Katafuchi et al., 2015). To further test this potential competition hypothesis, an AAV dose response study was also carried out. As shown in Fig. S3A, different amounts of injected AAV viral particles resulted in different amounts of plasma FGF21 levels. Effects on both body weight and fasting plasma glucose levels demonstrated a dose dependent response to FGF21 (Fig. S3B). Liver *Cyp7a1* expression and bile acid pool also demonstrated a dose dependent response (Fig. S3C). This dose dependency is also consistent with the expectation that antagonistic activity is more effective at higher FGF21 levels.

3.6. The C-terminal Tail of FGF21 is Unable to Regulate Body Weight and Glucose Metabolism, But is Sufficient to Increase Cyp7a1 Expression

Previous studies have shown that the βKlotho binding domain on FGF21 resides in its C-terminal portion, while the N-terminal domain is important for FGFR interaction and activation (Wu and Li, 2011). A FGF21 C-terminal fragment (from amino acid residues 138–181, termed FGF21CTD or CTD here) has been reported to be completely inactive on receptor signaling but is still able to bind βKlotho (Goetz et al., 2012). We, therefore, constructed an AAV to express this "inactive" FGF21, FGF21CTD, *in vivo*. If the hypothesis that FGF21 increases *Cyp7a1* expression by antagonizes FGF15/19 function on βKlotho/FGFR4 is correct, then FGF21CTD, due to its ability to bind βKlotho, should be able to inhibit FGF15/19 function and increase *Cyp7a1* expression while unable to activate any other function typically observed for FGF21. In addition, since FGF21-KO mice had only a mild phenotype and displayed no difference to wild type animals on body weight, glucose, insulin, and TG on a chow diet (Hotta et al., 2009), FGF21CTD is not expect to cause any significant impact on these metabolic parameters even if the endogenous FGF21 function is blocked by FGF21CTD. As shown in Fig. 3I, FGF15 and FGF21 injected mice showed the expected reduction in BW, glucose, plasma cholesterol and TG levels. In comparison, mice receiving FGF21CTD showed no changes in BW, glucose or plasma cholesterol and TG levels, but *Cyp7a1* expression in the liver was increased similar to wild type FGF21 (Fig. 3I). Thus, this data substantiates the hypothesis that FGF21 increases bile acid synthesis via inhibiting FGF15/19's function through βKlotho/FGFR4.

3.7. FGF21 Treatment Increases Colon Bile Acid Content in a Mouse Cholecystectomy Model

Since dysregulated FGF19 signaling and bile acid levels have been implicated in human conditions such as bile acid diarrhea, we wondered the potential consequence of FGF21 induced bile acid changes under these pathological conditions. The effect of FGF21 on bile acid transit through the enterohepatic circulation was thus tested in a mouse cholecystectomy model, mimicking a pathophysiological condition where the capacity to hold bile acid is reduced. One month post-surgery, animals were injected with AAV-EV or -FGF21. Two weeks post-injection, mice receiving FGF21 exhibited the expected reduction in BW, fasting blood glucose levels, and plasma TG levels (Fig. 4A). Similar to the wild type animals under normal chow and DIO conditions (Figs. 1 and 2), FGF21 treatment in cholecystectomized animals also increased bile acid pool (Fig. 4 and S2C). This increase in bile acid pool is not only reflected in the bile acid increases in the liver and small intestine, as is the case of wild type animals, there is also now a dramatic increase in the bile acid content in the colon (which was not observed in the wild type animals, compare Fig. 4B to Figs. 1 and 2). Expression analysis of key genes involved in bile acid synthesis and transport were also examined. Similar to the effects seen in wild type animals (Figs. 1C and 2C), FGF21 also increased *Cyp7a1* and *Cyp27a1* expression indicating increased bile acid synthesis, while no significant changes were observed with *Cyp7b1* and *Cyp8b1* (Fig. 4C). The bile acid transporters in liver and ileum were similarly changed compared to wild type animals (Fig. 4C). These results not only confirm the ability of FGF21 to increase bile acid pool via increased synthesis, but also demonstrate that when the storage capacity for bile acid is reduced, the increased bile acid pool can over flow into colon.

4. Discussion

FGF21 and FGF15/19 are two closely related molecules that play important roles in regulating glucose and energy homeostasis through a shared mechanism via the βKlotho/FGFR1c receptor complex (Zhang and Li, 2014). In addition, FGF19 is a key inhibitor of bile acid synthesis and pool size via direct engagement with liver βKlotho/FGFR4. Distinctly, FGF21 has yet to be linked to maintain bile acid homeostasis due to lack of activity on FGFR4. Here we provide data that over-expression of FGF21, contrary to FGF19, increases bile acid synthesis and pool size. Furthermore, we demonstrate that FGF21 achieves this not through direct activation of any FGFRs, but rather indirectly by inhibiting FGF19 function. We hypothesized that, since both FGF21 and FGF19 bind to overlapping sites on βKlotho, and require βKlotho binding for receptor function, FGF21 may be able to disrupt FGF19-βKlotho/FGFR4-mediated signaling. Our data corroborate this hypothesis by several lines of evidence: 1) although FGF21 does not activate FGFR4, its effects to induce *Cyp7a1* expression is dependent on FGFR4; 2) the ability of FGF21 to increase *Cyp7a1* expression observed in the chronic studies was not seen in the liver 5 hours post FGF21 injection, suggesting a potential indirect mechanism (Fig. 1); 3) FGF21 can directly inhibit FGF19 binding to and activation of βKlotho/FGFR4 complex *in vitro*, therefore may act as an antagonist to FGF19 mediated suppression of bile acid synthesis (Fig. 3); 4) an inactive FGF21, FGF21CTD, which binds βKlotho but does not signal or activate the βKlotho/FGFR complex, behaved similarly to native FGF21 in terms of bile acid regulation but failed to induce any effect on glucose or body weight regulation. Thus, together these results provide compelling evidence that the ability of FGF21 to increase bile acid synthesis and pool size is, at least in part, through its ability to antagonize the interaction of FGF19 with βKlotho/FGFR4, thereby modulating FGF19-mediated inhibition of bile acid synthesis.

Identifying this interplay between FGF21 and FGF19 to βKlotho revealed a novel regulatory mechanism to their function. Such crosstalk between different FGF molecules is not restricted to endocrine FGFs, a recent report also highlighted a regulatory mechanism via overlapping binding sites on FGF receptor between a paracrine FGF, FGF8, and βKlotho (Goetz et al., 2012). βKlotho binds the immunoglobulin-like domain III (D3) of the "c" splice isoform of FGFR1–3 and FGFR4. Intriguingly, this portion of the FGFR is also the binding site for FGF8, suggesting there could also be cross regulation between paracrine and endocrine FGF molecules. Therefore, in addition to the tissue specific expression of FGF receptors and co-receptors, competition between FGF molecules to co-receptor or receptors, or between FGFs and co-receptors to FGF receptors could serve as an additional layer of functional regulation under physiological or pathophysiological conditions *in vivo*.

Expression analysis was performed to further understand the effects of FGF21 on bile acid metabolism. As discussed above, the key gene involved in bile acid synthesis, *Cyp7a1*, was regulated in opposite

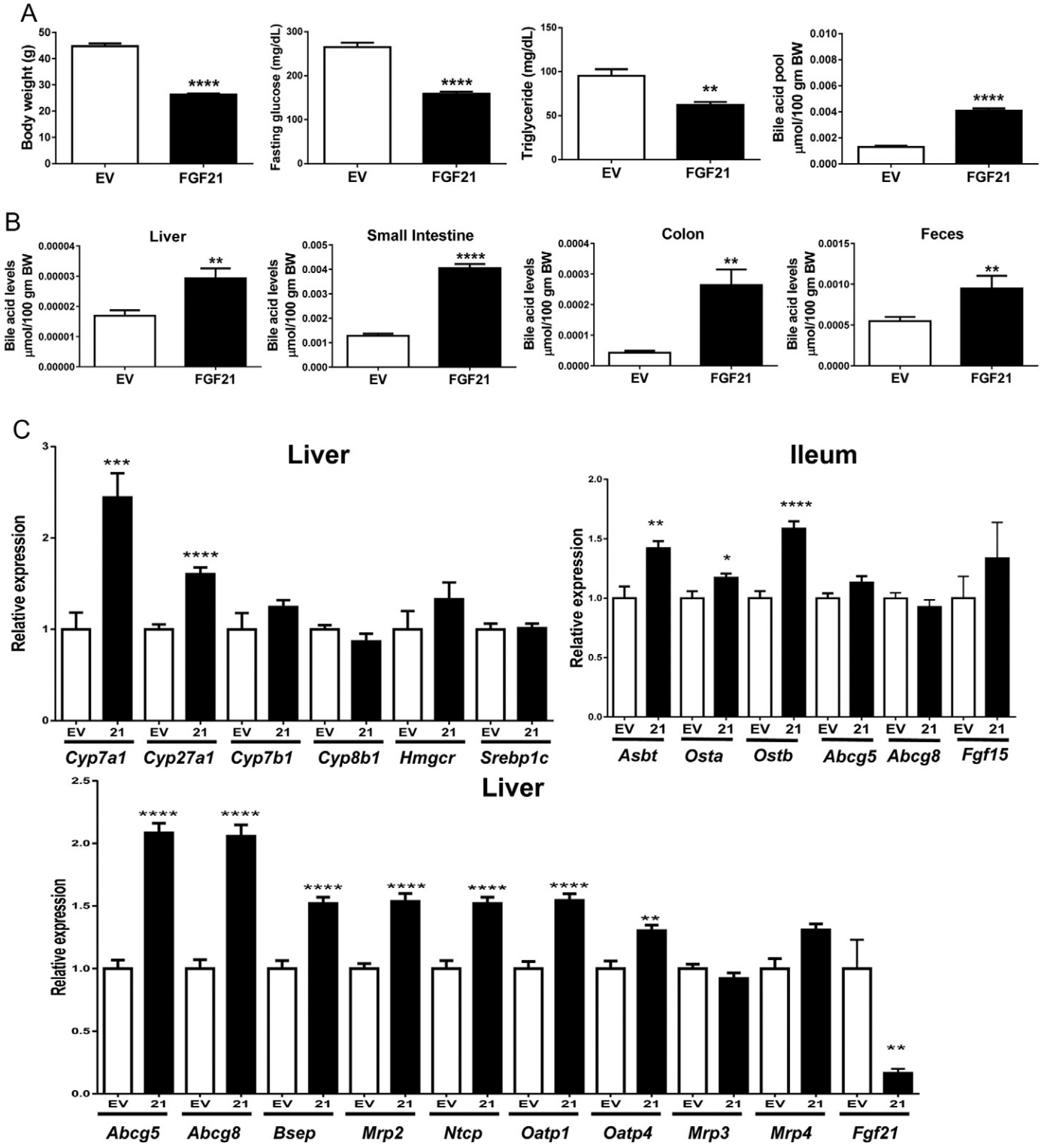

Fig. 4. FGF21 significantly increases colon bile acid regulation in cholecystectomized DIO animals. 16–18 week old C57BL/6 DIO animals underwent cholecystectomy surgery. One month post-surgery, animals were injected with AAV-EV or AAV-FGF21 (n = 8 each group). (A) Body weight, fasting glucose, and plasma triglyceride were significantly decreased at week 2 post AAV delivery. The total bile acid pool levels were significantly increased in animals treated with AAV-FGF21. (B) Liver, small intestine, colon and feces bile acid levels in animals treated with AAV-EV and AAV-FGF21 (n = 8 each group). (C) qPCR analysis of key enzymes in bile acid synthesis and transporters in the liver and ileum. mRNA abundance was normalized by housekeeping genes and is presented as relative expression. *$p < 0.05$, **$p < 0.01$, ***$p < 0.001$, ****$p < 0.0001$.

directions by FGF21 and FGF15/19. Similarly, the export pump on hepatocytes moving bile salts to the gallbladder, *Bsep*, is also increased in FGF21-treated animals but reduced in FGF15-treated animals, corresponding to the increased or reduced bile acid synthesis effects of these two molecules. FGF21 also increased *Cyp27a1* expression but was minimally affected by FGF15 treatment. However, while FGF21 and FGF15 regulated *Cyp7a1* and *Bsep* in opposite directions consistent with their observed effects on the bile acid pool, most of the other affected transporters were regulated similarly between FGF21 and FGF15. For example, the ileal transporter *Asbt*, and transporters involved in portal

bile acid reuptake into hepatocytes, *Ntcp*, *Oatp1*, and *Oatp4* were all up-regulated by both FGF21 and FGF15. In the chronically reduced bile acid pool conditions under FGF15 treatment, these increases might be a compensatory effect to reabsorb and preserve the remaining bile acid pool. However, the similar increases in the FGF21-treated group may argue either that increased bile acid flux itself may trigger increased re-uptake, or alternatively, that both FGF21 and FGF15 activated a common receptor(s) on liver and ileum directly or produced a common endocrine factor from another tissue that acted on liver and ileum to induce these increases.

The opposing effects of FGF21 and FGF15/19 on bile acid synthesis observed in our studies raises the question of whether FGF21 is an endogenous regulator of FGF15/19. It is interesting to note that, diabetic animals and humans have elevated bile acid pool and fecal bile acids with impaired FGF15/19 signaling or FGF15/19 resistance (Fu et al., 2012; Li et al., 2012; Bennion and Grundy, 1977). Coincidentally, serum FGF21 levels were also significantly elevated under these conditions while FGF19 levels may be reduced (Zhang et al., 2008; Li et al., 2011b; Hao et al., 2013; Gallego-Escuredo et al., 2015). In addition, the oscillating plasma FGF21 and FGF15/19 levels do not appear to coincide with each other, when FGF21 is high FGF15/19 is low and vice versa (Gallego-Escuredo et al., 2015; Yu et al., 2011; Lundasen et al., 2006). And lastly, since FGF21 is mainly produced in the liver, the local liver FGF21 levels may be significantly higher than plasma levels, raising the possibility that the interplay between endogenous FGF21 and FGF19 may exist. Future studies will be needed to address whether this antagonistic mechanism may indeed be important under physiological conditions for bile acid regulation. However, our results suggest that FGF21 may indeed antagonize FGF19 function on FGFR4 at least under certain pharmacological and supraphysiological conditions. Our results further show that in a cholecystectomy model, overexpression of FGF21 not only increased bile acid synthesis and bile acid pool size, but also with reduced capacity to hold bile acid in the absence of a gallbladder, more bile acid was observed transiting into the colon (Fig. 4). Since reduced FGF19 function, cholecystectomy, and increased bile acid flux into colon are risk factors for bile acid diarrhea in humans (Walters, 2014), clinical evaluation of FGF21 molecules especially in patients without a functional or intact gallbladder, should be monitored for changes to bile acid metabolism and diarrhea. Consistent with these arguments, a recent clinical study with a long acting FGF21 analog in human type 2 diabetes subjects where the plasma exposure of the FGF21 drug was significantly higher than the level measured in our AAV studies, the most frequent adverse events (AE) reported were diarrhea especially in high dose group (Talukdar et al., 2016). Although the authors did not described the mechanism for this AE nor clarified whether bile acid metabolism was affected in these subjects, it is interesting to speculate whether interference of the FGF19 pathway due to high FGF21 levels might have contributed to diarrhea. However, as the studies described in this report are all from overexpression of mouse FGF21 in rodent models, the relevance of these findings to humans will require direct assessment of bile acid metabolism in future clinical studies.

In conclusion, we identified a novel role for FGF21 in regulating bile acid homeostasis. Overexpression of FGF21 in mice leads to increased bile acid synthesis and bile acid pool size, at least in part, through antagonizing FGF15/19's ability to function through βKlotho/FGFR4. Therefore, pharmacological administration of FGF21, in addition to its anti-diabetic effects, may also impact bile acid homeostasis by blocking endogenous FGF15/19-regulated bile acid synthesis. These observations may have clinical significance as the FGF21 pathway continues to be explored for therapeutics.

Funding Sources and Conflict of Interest

The work is entirely funded by Amgen, Inc. Except YZ, all other authors are employees of Amgen, Inc.

Author Contributions

JZ, WR, and YL conceived and designed the experiments; JZ, JG, YG, JW, YZ, and KJL performed the experiments; JZ, JG, YG, JW, YZ, WR, and YL analyzed the data; JZ and YL wrote the manuscript. All authors reviewed the results and approved the final version of the manuscript.

Acknowledgments

We thank Nessa Hawkins, Grant Shimamoto, and Huiren Zhao for recombinant proteins and AAVs, we thank Jonitha Gardner and Ya-Wen Lu for technical support, we thank Mingyue Zhou, W. Scott Simonet and Steven A. Kliewer for helpful discussions, and we thank Ingrid Rulifson for editing this manuscript.

Appendix A. Supplementary data

Supplementary data to this article can be found online at http://dx.doi.org/10.1016/j.ebiom.2016.12.016.

References

Bennion, L.J., Grundy, S.M., 1977. Effects of diabetes mellitus on cholesterol metabolism in man. N. Engl. J. Med. 296, 1365–1371.
Coskun, T., Bina, H.A., Schneider, M.A., Dunbar, J.D., Hu, C.C., Chen, Y., Moller, D.E., Kharitonenkov, A., 2008. Fibroblast growth factor 21 corrects obesity in mice. Endocrinology 149, 6018–6027.
Ding, X., Boney-Montoya, J., Owen, B.M., Bookout, A.L., Coate, K.C., Mangelsdorf, D.J., Kliewer, S.A., 2012. betaKlotho is required for fibroblast growth factor 21 effects on growth and metabolism. Cell Metab. 16, 387–393.
Fu, L., John, L.M., Adams, S.H., Yu, X.X., Tomlinson, E., Renz, M., Williams, P.M., Soriano, R., Corpuz, R., Moffat, B., et al., 2004. Fibroblast growth factor 19 increases metabolic rate and reverses dietary and leptin-deficient diabetes. Endocrinology 145, 2594–2603.
Fu, T., Choi, S.E., Kim, D.H., Seok, S., Suino-Powell, K.M., Xu, H.E., Kemper, J.K., 2012. Aberrantly elevated microRNA-34a in obesity attenuates hepatic responses to FGF19 by targeting a membrane coreceptor beta-Klotho. Proc. Natl. Acad. Sci. U. S. A. 109, 16137–16142.
Gallego-Escuredo, J.M., Gomez-Ambrosi, J., Catalan, V., Domingo, P., Giralt, M., Fruhbeck, G., Villarroya, F., 2015. Opposite alterations in FGF21 and FGF19 levels and disturbed expression of the receptor machinery for endocrine FGFs in obese patients. Int. J. Obes. 39, 121–129.
Ge, H., Baribault, H., Vonderfecht, S., Lemon, B., Weiszmann, J., Gardner, J., Lee, K.J., Gupte, J., Mookherjee, P., Wang, M., et al., 2012. Characterization of a FGF19 variant with altered receptor specificity revealed a central role for FGFR1c in the regulation of glucose metabolism. PLoS One 7, e33603.
Ge, H., Zhang, J., Gong, Y., Gupte, J., Ye, J., Weiszmann, J., Samayoa, K., Coberly, S., Gardner, J., Wang, H., et al., 2014. Fibroblast growth factor receptor 4 (FGFR4) deficiency improves insulin resistance and glucose metabolism under diet-induced obesity conditions. J. Biol. Chem. 289, 30470–30480.
Goetz, R., Ohnishi, M., Ding, X., Kurosu, H., Wang, L., Akiyoshi, J., Ma, J., Gai, W., Sidis, Y., Pitteloud, N., et al., 2012. Klotho coreceptors inhibit signaling by paracrine fibroblast growth factor 8 subfamily ligands. Mol. Cell. Biol. 32, 1944–1954.
Hao, Y., Zhou, J., Zhou, M., Ma, X., Lu, Z., Gao, M., Pan, X., Tang, J., Bao, Y., Jia, W., 2013. Serum levels of fibroblast growth factor 19 are inversely associated with coronary artery disease in Chinese individuals. PLoS One 8, e72345.
Holt, J.A., Luo, G., Billin, A.N., Bisi, J., McNeill, Y.Y., Kozarsky, K.F., Donahee, M., Wang, D.Y., Mansfield, T.A., Kliewer, S.A., et al., 2003. Definition of a novel growth factor-dependent signal cascade for the suppression of bile acid biosynthesis. Genes Dev. 17, 1581–1591.
Hotta, Y., Nakamura, H., Konishi, M., Murata, Y., Takagi, H., Matsumura, S., Inoue, K., Fushiki, T., Itoh, N., 2009. Fibroblast growth factor 21 regulates lipolysis in white adipose tissue but is not required for ketogenesis and triglyceride clearance in liver. Endocrinology 150, 4625–4633.
Inagaki, T., Choi, M., Moschetta, A., Peng, L., Cummins, C.L., McDonald, J.G., Luo, G., Jones, S.A., Goodwin, B., Richardson, J.A., et al., 2005. Fibroblast growth factor 15 functions as an enterohepatic signal to regulate bile acid homeostasis. Cell Metab. 2, 217–225.
Ito, S., Fujimori, T., Furuya, A., Satoh, J., Nabeshima, Y., Nabeshima, Y., 2005. Impaired negative feedback suppression of bile acid synthesis in mice lacking betaKlotho. J. Clin. Invest. 115, 2202–2208.
Katafuchi, T., Esterhazy, D., Lemoff, A., Ding, X., Sondhi, V., Kliewer, S.A., Mirzaei, H., Mangelsdorf, D.J., 2015. Detection of FGF15 in plasma by stable isotope standards and capture by anti-peptide antibodies and targeted mass spectrometry. Cell Metab. 21, 898–904.
Kharitonenkov, A., Shiyanova, T.L., Koester, A., Ford, A.M., Micanovic, R., Galbreath, E.J., Sandusky, G.E., Hammond, L.J., Moyers, J.S., Owens, R.A., et al., 2005. FGF-21 as a novel metabolic regulator. J. Clin. Invest. 115, 1627–1635.
Kharitonenkov, A., Wroblewski, V.J., Koester, A., Chen, Y.F., Clutinger, C.K., Tigno, X.T., Hansen, B.C., Shanafelt, A.B., Etgen, G.J., 2007. The metabolic state of diabetic monkeys is regulated by fibroblast growth factor-21. Endocrinology 148, 774–781.

Kong, B., Wang, L., Chiang, J.Y., Zhang, Y., Klaassen, C.D., Guo, G.L., 2012. Mechanism of tissue-specific farnesoid X receptor in suppressing the expression of genes in bile-acid synthesis in mice. Hepatology 56, 1034–1043.

Kurosu, H., Choi, M., Ogawa, Y., Dickson, A.S., Goetz, R., Eliseenkova, A.V., Mohammadi, M., Rosenblatt, K.P., Kliewer, S.A., Kuro-o, M., 2007. Tissue-specific expression of betaKlotho and fibroblast growth factor (FGF) receptor isoforms determines metabolic activity of FGF19 and FGF21. J. Biol. Chem. 282, 26687–26695.

Li, T., Owsley, E., Matozel, M., Hsu, P., Novak, C.M., Chiang, J.Y., 2010. Transgenic expression of cholesterol 7alpha-hydroxylase in the liver prevents high-fat diet-induced obesity and insulin resistance in mice. Hepatology 52, 678–690.

Li, T., Matozel, M., Boehme, S., Kong, B., Nilsson, L.M., Guo, G., Ellis, E., Chiang, J.Y., 2011a. Overexpression of cholesterol 7alpha-hydroxylase promotes hepatic bile acid synthesis and secretion and maintains cholesterol homeostasis. Hepatology 53, 996–1006.

Li, X., Fan, X., Ren, F., Zhang, Y., Shen, C., Ren, G., Sun, J., Zhang, N., Wang, W., Ning, G., et al., 2011b. Serum FGF21 levels are increased in newly diagnosed type 2 diabetes with nonalcoholic fatty liver disease and associated with hsCRP levels independently. Diabetes Res. Clin. Pract. 93, 10–16.

Li, T., Francl, J.M., Boehme, S., Ochoa, A., Zhang, Y., Klaassen, C.D., Erickson, S.K., Chiang, J.Y., 2012. Glucose and insulin induction of bile acid synthesis: mechanisms and implication in diabetes and obesity. J. Biol. Chem. 287, 1861–1873.

Lin, B.C., Wang, M., Blackmore, C., Desnoyers, L.R., 2007. Liver-specific activities of FGF19 require Klotho beta. J. Biol. Chem. 282, 27277–27284.

Lundasen, T., Galman, C., Angelin, B., Rudling, M., 2006. Circulating intestinal fibroblast growth factor 19 has a pronounced diurnal variation and modulates hepatic bile acid synthesis in man. J. Intern. Med. 260, 530–536.

Myant, N.B., Mitropoulos, K.A., 1977. Cholesterol 7 alpha-hydroxylase. J. Lipid Res. 18, 135–153.

Ogawa, Y., Kurosu, H., Yamamoto, M., Nandi, A., Rosenblatt, K.P., Goetz, R., Eliseenkova, A.V., Mohammadi, M., Kuro-o, M., 2007. BetaKlotho is required for metabolic activity of fibroblast growth factor 21. Proc. Natl. Acad. Sci. U. S. A. 104, 7432–7437.

Russell, D.W., Setchell, K.D., 1992. Bile acid biosynthesis. Biochemistry 31, 4737–4749.

Talukdar, S., Zhou, Y., Li, D., Rossulek, M., Dong, J., Somayaji, V., Weng, Y., Clark, R., Lanba, A., Owen, B.M., et al., 2016. A long-acting FGF21 molecule, PF-05231023, decreases body weight and improves lipid profile in non-human primates and type 2 diabetic subjects. Cell Metab. 23, 427–440.

Thomas, C., Pellicciari, R., Pruzanski, M., Auwerx, J., Schoonjans, K., 2008. Targeting bile-acid signalling for metabolic diseases. Nat. Rev. Drug Discov. 7, 678–693.

Tomlinson, E., Fu, L., John, L., Hultgren, B., Huang, X., Renz, M., Stephan, J.P., Tsai, S.P., Powell-Braxton, L., French, D., et al., 2002. Transgenic mice expressing human fibroblast growth factor-19 display increased metabolic rate and decreased adiposity. Endocrinology 143, 1741–1747.

Walters, J.R., 2014. Bile acid diarrhoea and FGF19: new views on diagnosis, pathogenesis and therapy. Nat. Rev. Gastroenterol. Hepatol. 11, 426–434.

Wu, X., Li, Y., 2011. Therapeutic utilities of fibroblast growth factor 19. Expert Opin. Ther. Targets 15, 1307–1316.

Wu, X., Ge, H., Gupte, J., Weiszmann, J., Shimamoto, G., Stevens, J., Hawkins, N., Lemon, B., Shen, W., Xu, J., et al., 2007. Co-receptor requirements for fibroblast growth factor-19 signaling. J. Biol. Chem. 282, 29069–29072.

Wu, X., Lemon, B., Li, X., Gupte, J., Weiszmann, J., Stevens, J., Hawkins, N., Shen, W., Lindberg, R., Chen, J.L., et al., 2008. C-terminal tail of FGF19 determines its specificity toward Klotho co-receptors. J. Biol. Chem. 283, 33304–33309.

Wu, X., Ge, H., Lemon, B., Weiszmann, J., Gupte, J., Hawkins, N., Li, X., Tang, J., Lindberg, R., Li, Y., 2009. Selective activation of FGFR4 by an FGF19 variant does not improve glucose metabolism in Ob/Ob mice. Proc. Natl. Acad. Sci. U. S. A. 106, 14379–14384.

Wu, X., Ge, H., Lemon, B., Vonderfecht, S., Weiszmann, J., Hecht, R., Gupte, J., Hager, T., Wang, Z., Lindberg, R., et al., 2010. FGF19-induced hepatocyte proliferation is mediated through FGFR4 activation. J. Biol. Chem. 285, 5165–5170.

Wu, A.L., Coulter, S., Liddle, C., Wong, A., Eastham-Anderson, J., French, D.M., Peterson, A.S., Sonoda, J., 2011. FGF19 regulates cell proliferation, glucose and bile acid metabolism via FGFR4-dependent and independent pathways. PLoS One 6, e17868.

Xu, J., Lloyd, D.J., Hale, C., Stanislaus, S., Chen, M., Sivits, G., Vonderfecht, S., Hecht, R., Li, Y.S., Lindberg, R.A., et al., 2009a. Fibroblast growth factor 21 reverses hepatic steatosis, increases energy expenditure, and improves insulin sensitivity in diet-induced obese mice. Diabetes 58, 250–259.

Xu, J., Stanislaus, S., Chinookoswong, N., Lau, Y.Y., Hager, T., Patel, J., Ge, H., Weiszmann, J., Lu, S.C., Graham, M., et al., 2009b. Acute glucose-lowering and insulin-sensitizing action of FGF21 in insulin-resistant mouse models–association with liver and adipose tissue effects. Am. J. Physiol. Endocrinol. Metab. 297, E1105–E1114.

Yang, C., Jin, C., Li, X., Wang, F., McKeehan, W.L., Luo, Y., 2012. Differential specificity of endocrine FGF19 and FGF21 to FGFR1 and FGFR4 in complex with KLB. PLoS One 7, e33870.

Yu, C., Wang, F., Kan, M., Jin, C., Jones, R.B., Weinstein, M., Deng, C.X., McKeehan, W.L., 2000. Elevated cholesterol metabolism and bile acid synthesis in mice lacking membrane tyrosine kinase receptor FGFR4. J. Biol. Chem. 275, 15482–15489.

Yu, H., Xia, F., Lam, K.S., Wang, Y., Bao, Y., Zhang, J., Gu, Y., Zhou, P., Lu, J., Jia, W., et al., 2011. Circadian rhythm of circulating fibroblast growth factor 21 is related to diurnal changes in fatty acids in humans. Clin. Chem. 57, 691–700.

Zhang, J., Li, Y., 2014. Fibroblast growth factor 21, the endocrine FGF pathway and novel treatments for metabolic syndrome. Drug Discov. Today 19, 579–589.

Zhang, X., Yeung, D.C., Karpisek, M., Stejskal, D., Zhou, Z.G., Liu, F., Wong, R.L., Chow, W.S., Tso, A.W., Lam, K.S., et al., 2008. Serum FGF21 levels are increased in obesity and are independently associated with the metabolic syndrome in humans. Diabetes 57, 1246–1253.